Supporting Information

Construction of $NaREF_4$-based Binary and Bilayer Nanocrystal Assemblies

Tao Zheng, Ling-Dong Sun,* Jia-Cai Zhou, Wei Feng, Chao Zhang, and Chun-Hua Yan*

Beijing National Laboratory for Molecular Sciences, State Key Laboratory of Rare Earth Materials Chemistry and Applications, PKU-HKU Joint Lab on Rare Earth Materials and Bioinorganic Chemistry, College of Chemistry and Molecular Engineering, Peking University, Beijing 100871, China.

Fax: +86 10 6275 4179; Tel: +86 10 6275 4179;
E-mail: sun@pku.edu.cn (L. D. Sun), yan@pku.edu.cn (C. H. Yan)

Experimentation

1. Chemicals. Schlenk line system was used in the nanocrystal (NC) synthesis. Oleic acid (OA; >90%, Sigma-Aldrich), oleylamine (OM; >80%, Acros), 1-octadecene (ODE; >90%, Acros), trifluoroacetate acid (99%, Acros), trifluoroacetic acid sodium salt (99%, Acros), selenium powders (Se; G. R. grade), cadmium oxide (CdO; A. R. grade), chloroauric acid hydrated ($HAuCl_4\cdot 4H_2O$; A. R. grade, SCRC), dodecyldimethylammonium bromide (DDAB; G. R. grade, TCI), sodium borohydride ($NaBH_4$; >98%, A. R. grade), ethanol (A. R. grade), *n*-hexane (A. R. grade), cyclohexane (A. R. grade), toluene (A. R. grade), and diethylene glycol (A. R. grade) were used as received without further purification. $RE(CF_3COO)_3$ (RE = Y, Yb, Gd, Er, Tm) and $Ca(CF_3COO)_2$ were prepared from the corresponding lanthanide oxides and trichloroacetic acid. All the NCs were synthesized by using standard air-free procedures.

2. Nanocrystal synthesis. All NCs used as building blocks for BNSLs in this work (see Table S1) were synthesized in nonpolar solvents and stabilized with amphiphilic molecules that served as capping ligands according to the previous reported methods (or modified methods).[S1-S5] Detailed information on the preparation of these NCs is given below.

2.1 Synthesis of $NaYF_4$:Yb,Er, $NaYF_4$:Yb,Tm and $NaGdF_4$:Yb,Er. A given amount of $RE(CF_3COO)_3$ (1 mmol) and CF_3COONa (1 mmol) was added into a mixture of 40 mmol of OA, OM and ODE (the molar ratio was 1:1:2) in a three-necked flask (100 mL) at room temperature. The slurry was then heated to 120 °C to remove water and oxygen with vigorous magnetic stirring under vacuum for several minutes in a temperature-controlled electromantle, and thus to form an optically transparent solution. The solution was heated to 310 °C at a heating rate of 15 °C/min and kept for 30 min under a N_2 atmosphere. After cooling to room temperature, the nanoparticles (NPs) were precipitated by adding excess amount of absolute ethanol into the reacted solution, and then collected by centrifugation. Then the product was redispersed in 10 mL of cyclohexane. The concentration of $NaGdF_4$:Yb,Er NCs was *ca.* 2×10^{16} NPs/mL (8 mg/mL).

2.2 Synthesis of $NaYF_4$:Yb,Tm@CaF_2 and hexagonal $NaYF_4$:Yb,Er UCNCs. The as-prepared $NaYF_4$:Yb,Tm UCNCs was redispersed in a 40 mmol of OA/ODE mixture with the molar ratio of 1:1, and an extra 4 mmol of $Ca(CF_3COO)_2$ was added. Then, the slurry was heated to 120 °C to remove water and oxygen with vigorous magnetic stirring under vacuum for several minutes in a temperature-controlled electromantle to form an optically transparent solution. The solution was heated to 310 °C at a heating rate of 15 °C/min and kept for 30 min under a N_2 atmosphere. On cooling to room temperature, the NCs were precipitated by adding excess amount of absolute ethanol into the reacted solution, and then collected by centrifugation. Then the product was redispersed in 10 mL of cyclohexane. The concentration of α-$NaYF_4$:Yb,Tm@CaF_2 NCs was *ca.* 3 × 10^{15} NPs/mL (11 mg/mL). With the similar method, while replacing as-prepared $NaYF_4$:Yb,Tm UCNCs with $NaYF_4$:Yb,Er UCNCs, 4 mmol of $Ca(CF_3COO)_2$ with 1 mmol of CF_3COONa, and maintaining the reaction temperature at 330 °C for 30 min, hexagonal $NaYF_4$:Yb,Er UCNCs (d = 27.0±0.7 nm) can be synthesized, too. The concentration was *ca.* 1 × 10^{14} NPs/mL (4 mg/mL).

2.3 Synthesis of CdSe NCs. In a typical synthesis, 0.032 g (0.40 mmol) of Se powder and 5.05 g of ODE were loaded into a three-necked flask (100 mL), and then heated to 280 °C for half an hour to get an apparent clear yellow solution. 0.32 g (2.5 mmol) of CdO, 2.01 g of OA, and 2.52 g of ODE were mixed together in a three-necked flask (100 mL) and heated to 120 °C to get a transparent solution, and then it was swiftly added to the Se stock solution. The temperature originally dropped and then quickly rose to about 280 °C by adjusting the power of the heating mantle. The temperature adjusted process can be finished in 1 min. During the whole reaction process, the temperature was maintained at 280 °C for the growth of the NCs. After about 10 min of reaction time, the flask was removed out of the heating mantle. Ethanol was added to the reactive solution to precipitate the NCs, and then the NCs were collected by centrifugation. Finally, the CdSe NCs were redispersed in 10 mL of *n*-hexane. The concentration of CdSe NCs was *ca.* 3 × 10^{15} NPs/mL (0.9 mg/mL).

2.4 Synthesis of 1-dodecanethiol-stabilized Au NCs. In a typical synthesis, 0.040 g of $HAuCl_4 \cdot 4H_2O$ was dissolved in 10 mL of toluene with ultrasonication in the presence of 0.0931 g of dodecyldimethylammonium bromide (DDAB). Then, 40 μL of 9.4 mol/L aqueous solution of $NaBH_4$ (mixture of 0.356g of $NaBH_4$ and 1 mL of icy water) was added drop-wise to the solution of metal salt with vigorous stirring. After 20min stirring, 0.8 mL of 1-dodecanethiol was added and the stirring was continued for five more minutes. The NCs were precipitated by adding excess absolute ethanol, and the solid was redispersed in 10 mL of toluene in the presence of 0.8 mL of 1-dodecanethiol. The concentration of 1-dodecanethiol-stabilized Au NCs was *ca.* 5 × 10^{14} NPs/mL (0.6 mg/mL).

2.5 Synthesis of OM-stabilized Au NCs. OM-stabilized Au NCs were obtained with $HAuCl_4 \cdot 4H_2O$ as precursor and OM as solvent as well as reductant. 0.025 mmol of $HAuCl_4 \cdot 4H_2O$ was dissolved in 10 g of OM through sonication, and the resulting solution was heated to 140 °C for several minutes until the color of the solution changed from yellow to purple. The as-precipitated NPs were precipitated by adding excess amount of absolute ethanol, and the solid was redispersed in 10 mL of toluene. The concentration of OM-stabilized Au NCs was *ca.* 2 × 10^{13} NPs/mL (0.3 mg/mL).

3. Self-assembly methods. All BNSLs we obtained in this work (see Table S2) were constructed by evaporation-induced self-assembly (EISA) or co-crystallization of multicomponent NCs at the liquid-air interface method.[S6,S7]

3.1.1 Method I: EISA. In a typical assembly process for an AlB_2-type BNSL, we mixed a 30 μL *n*-hexane solution of 4.5 nm CdSe NCs (*ca.* 3 × 10^{13} NPs/mL, 9 μg/mL) with a 30 μL cyclohexane solution of 6.0 nm $NaGdF_4$:Yb,Er NCs (*ca.* 3 × 10^{14} NPs/mL, 0.2 mg/mL) in a centrifuge tube. Then, 15 μL of the mixed colloidal solution of NCs was dispensed on a carbon-coated copper grid, which was placed on a clean silicon wafer. Then, the solvent was evaporated under ambient condition at room temperature to get BNSLs.

3.1.2 Method II: co-crystallization of multicomponent NCs at the liquid-air interface. In a typical assembly process for a NaCl-type BNSL, we mixed a 150 μL toluene solution of 4.8

nm Au NCs (*ca.* 1×10^{14} NPs/mL, 0.1 mg/mL) with a 50 μL cyclohexane solution of 12.5 nm α-$NaYF_4$:Yb,Tm@CaF_2 NCs (*ca.* 3×10^{14} NPs/mL, 1.1 mg/mL) in a centrifuge tube. Then, 20 μL of the mixed colloidal solution of NCs was spread on the surface of diethylene glycol (DEG) in a centrifuge tube (1.5 mL), which was covered with a glass slide to allow hexane and toluene to evaporate through the gaps between the tube surface and the glass slide under ambient condition at room temperature. After complete evaporation, a solid membrane formed and floated on the surface of DEG. The floating films were transferred onto a carbon-coated coordinate copper grid by the Langmuir-Schaefer method.[S8] Subsequent drying was performed in a vacuum drying oven to remove residual DEG at 65 °C.

3.2 Construction of monolayer and bilayer films. As a typical procedure, a 210 μL cyclohexane solution of 22.1 nm $NaYF_4$:Yb,Er NCs (*ca.* 5×10^{12} NPs/mL, 0.1 mg/mL) was spread on the surface of diethylene glycol (DEG) in a Teflon well (with its upper surface area *ca.* 11 cm^2) under ambient conditions. After complete evaporation for *ca.* 10 min, a solid membrane formed and floated on the surface of DEG. The floating films were transferred onto a carbon-coated coordinate copper grid by the Langmuir-Schaefer method. Subsequent drying was performed in a vacuum drying oven to remove residual DEG at 65 °C. With sequential transferring and drying of other component monolayers, bilayer assemblies were constructed.

Instrumentation

1. TEM, SAED & EDS. For TEM characterization, the constructed BNSLs, monolayer and bilayer films were collected on transmission electron microscopy (TEM) carbon-coated copper grids, coordinate copper grids or holey copper grids. TEM images, selected area electronic diffraction (SAED) and energy dispersive X-ray spectroscopy (EDS) analyses were performed on a JEOL JEM-2100 TEM and a JEOL JEM-2100F TEM operating at 200 kV. The coordinate copper grids also play the role in positioning. To identify the structures of the observed BNSLs, we built 3D structural models using Accelrys MS Studio 4.3. The TEM images were compared with simulated projections to match the symmetry of our superlattices. We also performed a comparison of the 2D FFT images of the simulated projections to ensure consistency.

2. ICP-AES. Inductively coupled plasma-atomic emission spectrometry (ICP-AES) characterization was performed with a Leeman Profile SPEC.

3. UC emission spectra and luminescence imaging. UC emission spectra of AlB_2-type BNSL which is composed of 10.9 nm Au and 27.0 nm $NaYF_4$:Yb,Er and corresponding 27.0 nm $NaYF_4$:Yb,Er monolayer are measured with LabRAM HR-800 Raman microscope (HORIBA, Jobin Yvon) equipped with a 3D automatically movable platform and an external 980 nm diode laser irradiated by optical fiber (oblique illumination). UC luminescence imaging of monolayer and bilayer films was performed on a Nikon A1R MP laser scanning confocal microscope equipped with Mai Tai HP DeepSee laser, standard 4-channel detector and spectral detector (25 PMT channels, 10 nm wavelength resolutions). Under the 970 nm excitation, the UC luminescence spectral images were acquired with spectral detector and processed using Nikon NIS-Elements Advanced Research software. For $NaYF_4$:Yb,Tm@CaF_2 UCNCs, the four channels between 450 nm and 490 nm were merged as the blue emission. For $NaYF_4$:Yb,Er UCNCs, the channel 550 – 560 nm were used for green emission detection. Furthermore, Nikon NIS-Elements Advanced Research software was used to show the UC luminescent spectra of the selected areas.

Supplementary Data

Table S1 The as-prepared NCs used as building blocks for BNSLs

Building blocks	Particle size (d) /nm	std.%	Capping ligands	Effective size ($d_{effective}$)* /nm
CdSe	4.5±0.4	9	OA	7.8
$NaGdF_4$:Yb,Er	6.0±0.5	8	OA	9.2
$NaYF_4$:Yb,Er	27.0±0.7	3	OA	30.5
$NaYF_4$:Yb,Tm@CaF_2	12.5 ± 0.9	7	OA	13.9
Au	4.8±0.3	6	1-dodecanethiol	6.3
Au	10.9±2.2	20	OM	13.5

* Defined as $d_{effective} = d_{core} + 2l_{shell}$, here d_{core} and l_{shell} are the diameter of the NC core and the length of the capping ligand, respectively. In our work, l_{shell} is estimated by the interparticle distance in the close packed 2D nanoparticle superlattices.

Table S2 Effective size ratio and superlattice structures of the as-constructed BNSLs

Building blocks	Effective size ratio (γ)	Superlattice structures
4.5 nm CdSe and 27.0 nm $NaYF_4$:Yb,Er	0.26	AB_2-type BNSL monolayer
10.9 nm Au and 27.0 nm $NaYF_4$:Yb,Er	0.44	AlB_2
10.9 nm Au and 27.0 nm $NaYF_4$:Yb,Er	0.44	$CaCu_5$
10.9 nm Au and 27.0 nm $NaYF_4$:Yb,Er	0.44	NaCl
10.9 nm Au and 27.0 nm $NaYF_4$:Yb,Er	0.44	A_2B_3-type BNSL bilayer
4.8 nm Au and 12.5 nm $NaYF_4$:Yb,Tm@CaF_2	0.45	NaCl
4.5 nm CdSe and 6.0 nm $NaGdF_4$:Yb,Er	0.85	AlB_2

Table S3 Calculated* molar ratio of [Gd]/[Cd] in AlB_2-type BNSL combined with 4.5 nm CdSe and 6.0 nm $NaGdF_4$:Yb,Er with different layers

Layer contents	Molar ratio of [Gd]/[Cd]
1 layer of $NaGdF_4$:Yb,Er + 1 layer of CdSe	0.78
1 layer of $NaGdF_4$:Yb,Er + 2 layers of CdSe	0.39
2 layers of $NaGdF_4$:Yb,Er + 1 layer of CdSe	1.6
2 layers of $NaGdF_4$:Yb,Er + 2 layers of CdSe	0.78
2 layers of $NaGdF_4$:Yb,Er + 3 layers of CdSe	0.52
3 layers of $NaGdF_4$:Yb,Er + 2 layers of CdSe	1.17
3 layers of $NaGdF_4$:Yb,Er + 3 layers of CdSe	0.78
3 layers of $NaGdF_4$:Yb,Er + 4 layers of CdSe	0.59
4 layers of $NaGdF_4$:Yb,Er + 3 layers of CdSe	1.04
…	…
n layers of $NaGdF_4$:Yb,Er + n layers of CdSe	0.78

*The derivation process:

$d(CdSe) = 4.5 \times 10^{-7}$ cm, $d(NaGdF_4:Yb,Er) = 6.0 \times 10^{-7}$ cm, $M_w(CdSe) = 191.4\ g\cdot mol^{-1}$, $M_w(NaGdF_4:Yb,Er) = 259.6\ g\cdot mol^{-1}$, $\rho(CdSe) = 5.66\ g\cdot cm^{-3}$, $\rho(NaGdF_4:Yb,Er) = 5.06\ g\cdot cm^{-3}$,

When BNSL is composed of "*m* layer of $NaGdF_4$:Yb,Er and *n* layer of CdSe", the molar ratio of [Gd]/[Cd]:

$n[Gd]/n[Cd] = m\cdot[1/6\pi\cdot d(NaGdF_4:Yb,Er)^3\cdot\rho(NaGdF_4:Yb,Er)\cdot M_w(NaGdF_4:Yb,Er)^{-1}]/\mathbf{2}n\cdot[1/6\,\pi\cdot d(CdSe)^3\cdot\rho(CdSe)\cdot M_w(CdSe)^{-1}] = 0.78m/n$

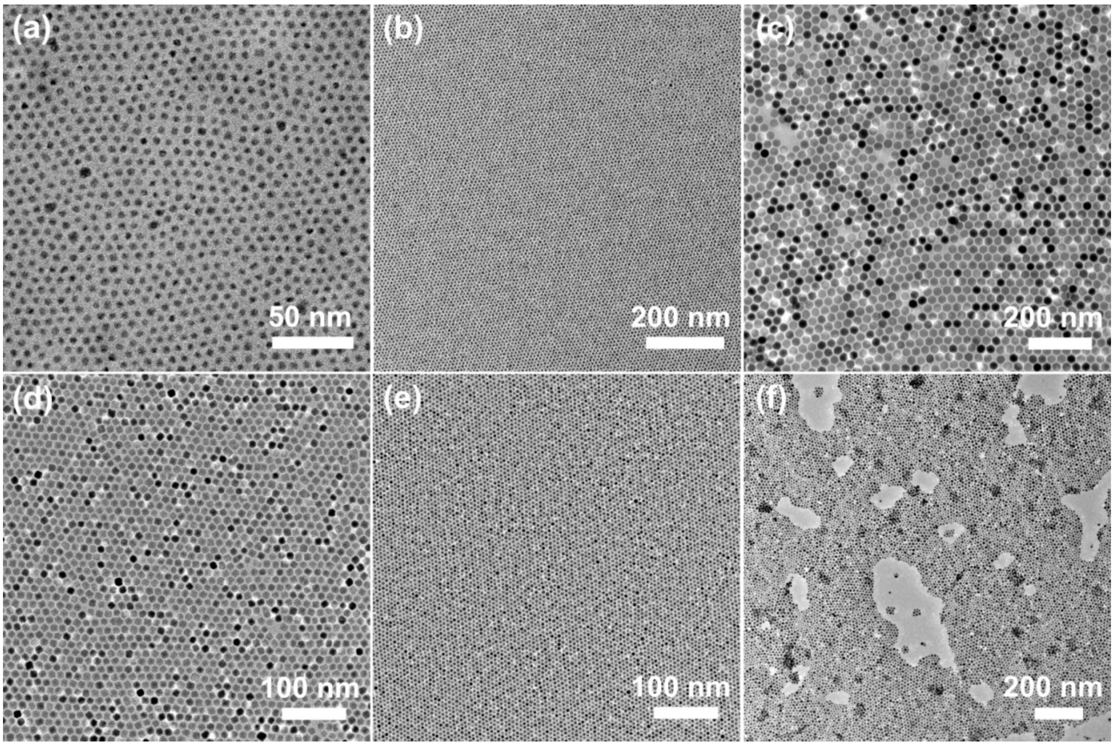

Figure S1 TEM images of the as-prepared NCs used as building blocks for BNSLs: (a) 4.5 nm CdSe, (b) 6.0 nm $NaGdF_4$:Yb,Er, (c) 27.0 nm $NaYF_4$:Yb,Er, (d) 12.5 nm $NaYF_4$:Yb,Tm@CaF_2, (e) 4.8 nm Au NCs, and (f) 10.9 nm Au NCs.

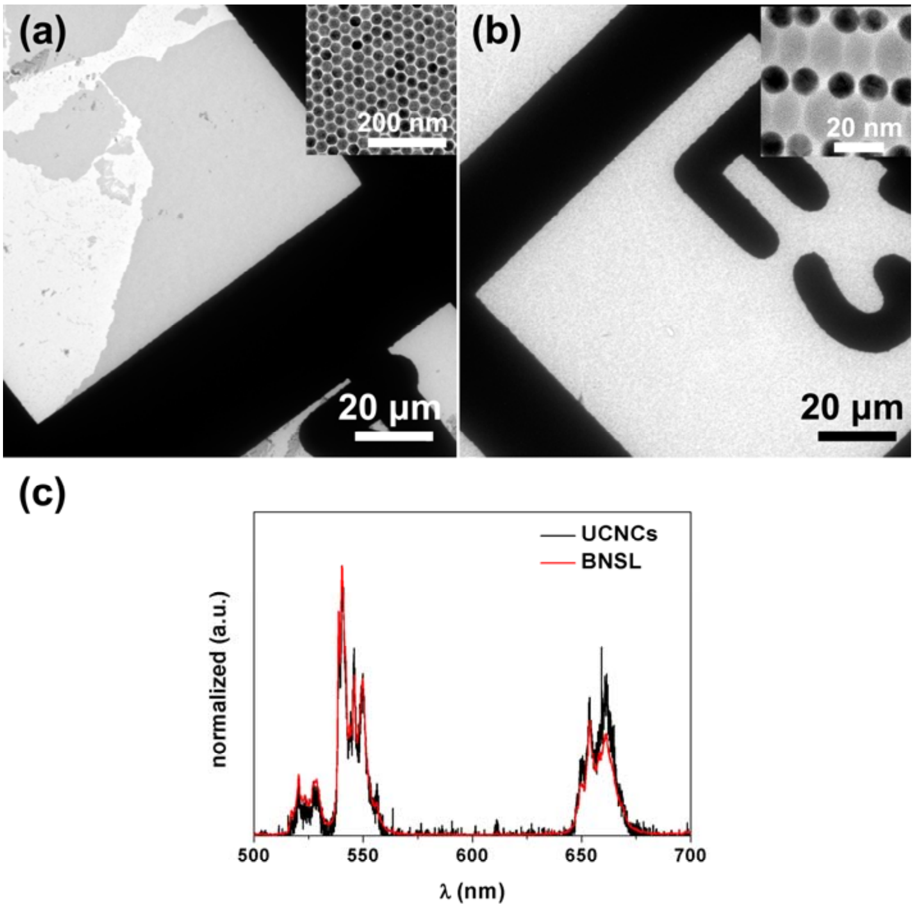

Figure S2 TEM images of (a) 27.0 nm $NaYF_4$:Yb,Er monolayer (upper inset, magnified view) , (b) AlB_2-type BNSL combined with 10.9 nm Au and 27.0 nm $NaYF_4$:Yb,Er as shown in Fig. 1b (upper inset, magnified view), (c) the corresponding UC emission spectra under 980 nm laser excitation.

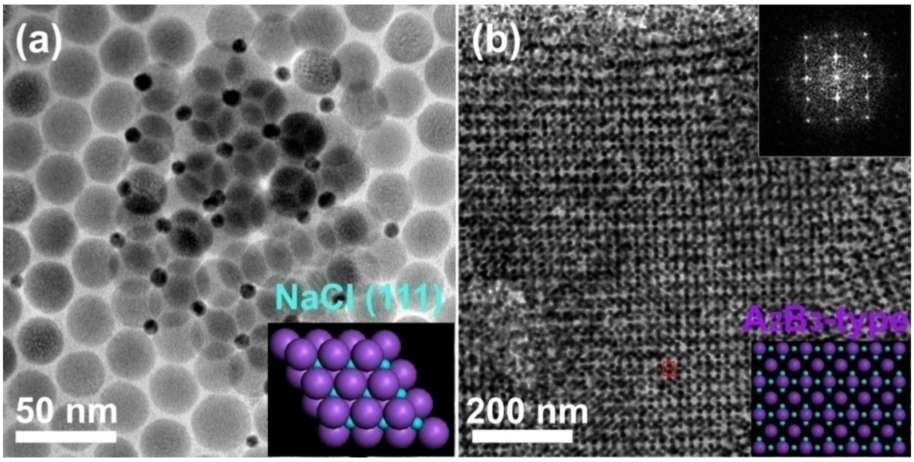

Figure S3 TEM images, FFT images (upper inset) and structural models (bottom inset) of (a) AB-type superlattices isostructural with NaCl, and (b) A_2B_3-type BNSL bilayer for the combination of 10.9 nm Au and 27.0 nm $NaYF_4$:Yb,Er. The red rectangle denotes an A_2B_3-type unit cell.

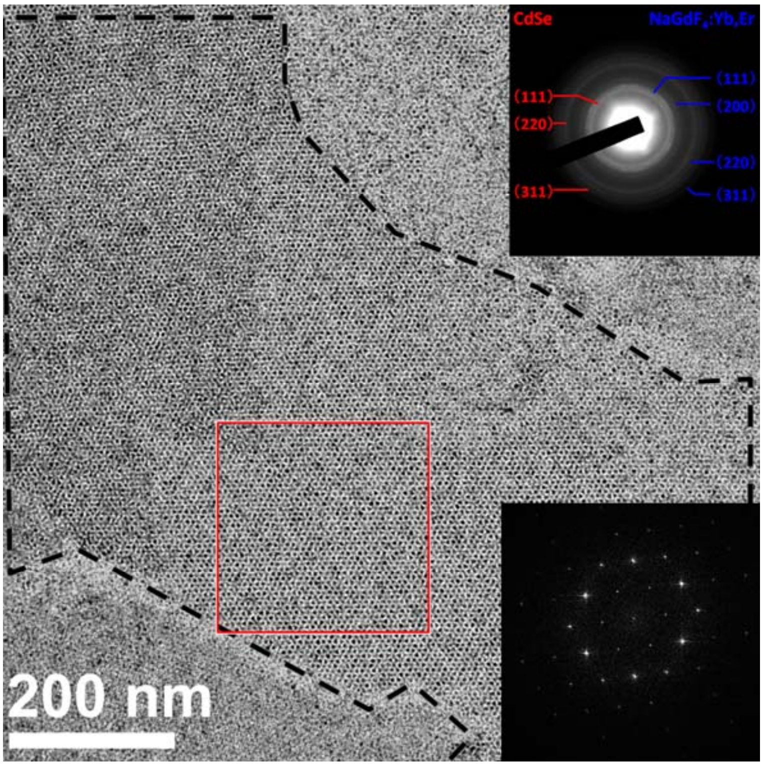

Figure S4 TEM image of AlB$_2$-type BNSL combined with 4.5 nm CdSe and 6.0 nm NaGdF$_4$:Yb,Er (upper inset, SAED pattern; bottom inset, FFT). The red rectangle shows the region selected for FFT.

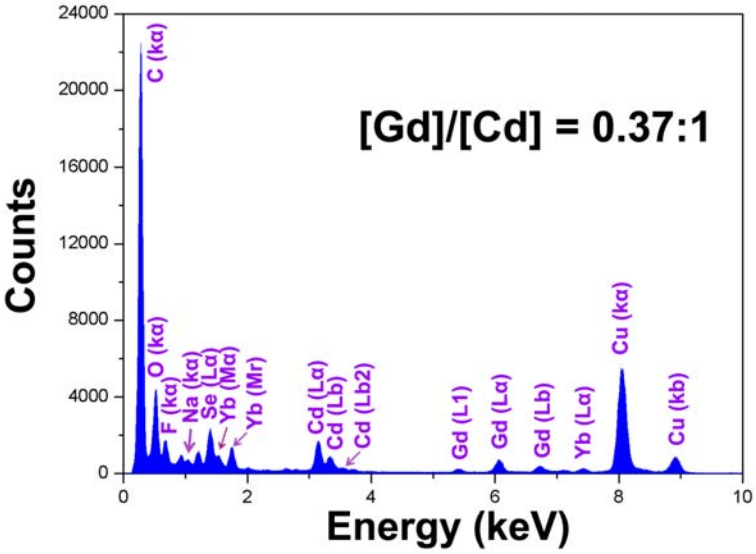

Figure S5 Corresponding EDS spectrum of AlB$_2$-type BNSL in Fig. 2b. The molar ratio of [Gd]/[Cd] is 0.37. The AlB$_2$-type BNSL may be composed of 1 layer of NaGdF$_4$:Yb,Er and 2 layers of CdSe, referring to Table S3.

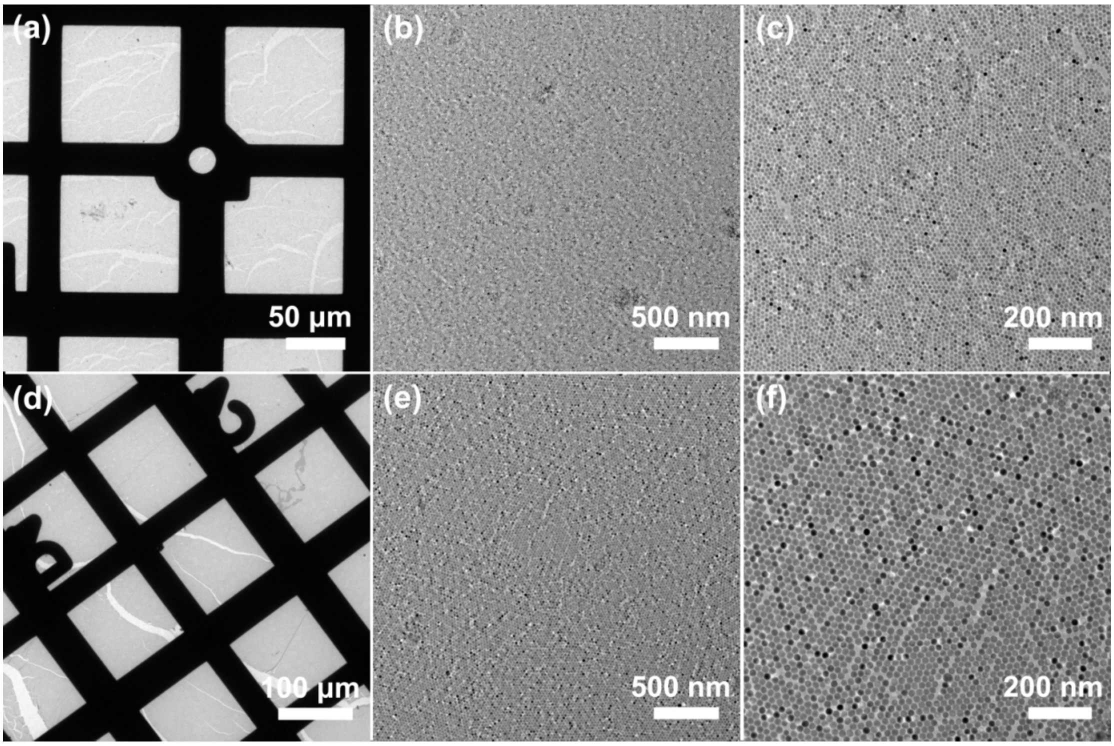

Figure S6 Gradually zoom-in TEM images of monolayers of 12.5nm $NaYF_4$:Yb,Tm@CaF_2: (a) 80×, (b) 8000×, (c) 20k×, and 22.1 nm $NaYF_4$:Yb,Er: (d) 50×, (e) 8000×, (f) 20k×

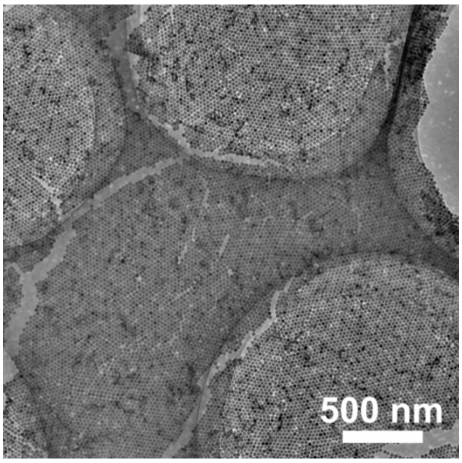

Figure S7 TEM image of a free-standing monolayer film consisting of 22.1 nm $NaYF_4$:Yb,Er suspended in the hole.

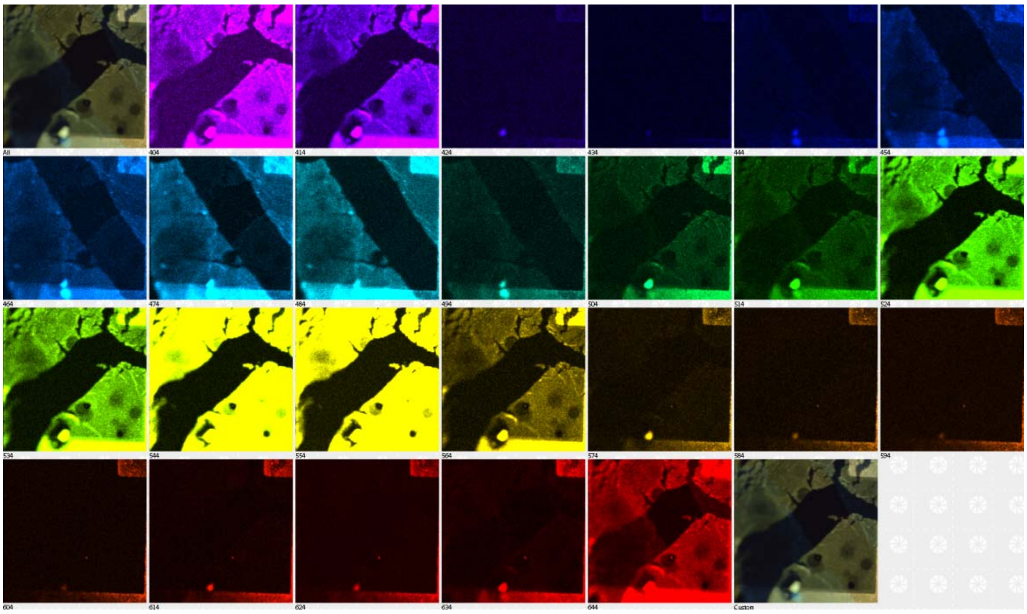

Figure S8 Full 25-channel false-colored UC emissions of bilayer assembly of $NaYF_4$:Yb,Tm@CaF_2 and $NaYF_4$:Yb,Er.

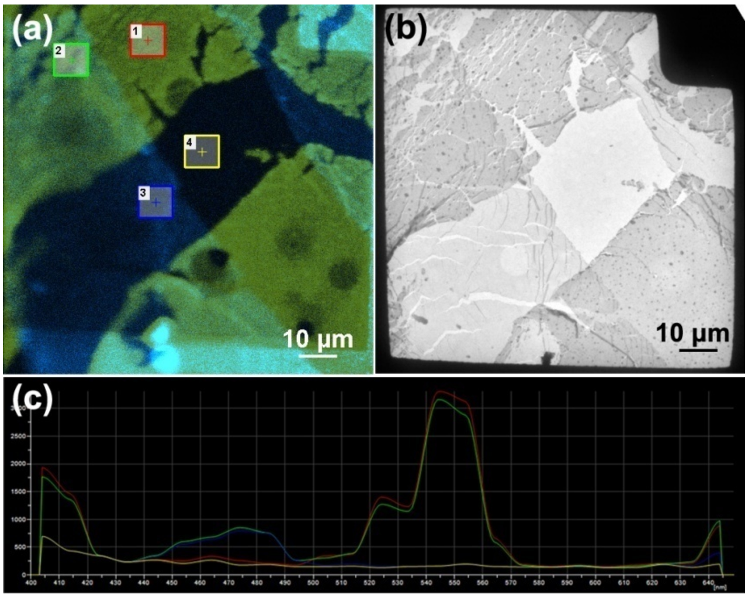

Figure S9 (a) False-colored UC emissions, (b) the correlated TEM image, (c) UC emission spectrum of ROI (region of interest) of 1 ~ 4 in (a). ROI-1: $NaYF_4$:Yb,Er monolayer, ROI-2: bilayer assembly, ROI-3: $NaYF_4$:Yb,Tm@CaF_2 monolayer, ROI-4: scarcely any nanoparticles

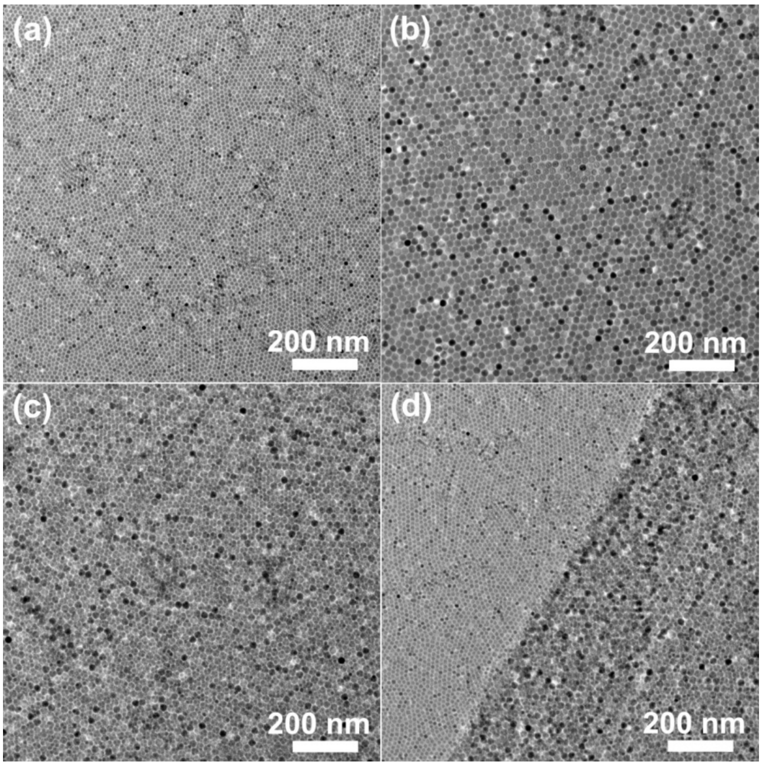

Figure S10 TEM images of the typical regions in Fig. S9b: (a) $NaYF_4$:Yb,Tm@CaF_2 monolayer, (b) $NaYF_4$:Yb,Er monolayer, (c) bilayer assembly of $NaYF_4$:Yb,Er and $NaYF_4$:Yb,Tm@CaF_2, and (d) the boundary between $NaYF_4$:Yb,Tm@CaF_2 monolayer and $NaYF_4$:Yb,Tm@CaF_2/$NaYF_4$:Yb,Er bilayer.

References

S1. H. X. Mai, Y. W. Zhang, R. Si, Z. G. Yan, L. D. Sun, L. P. You and C. H. Yan, *J. Am. Chem. Soc.*, 2006, **128**, 6426.

S2. Y. F. Wang, L. D. Sun, J. W. Xiao, W. Feng, J. C. Zhou, J. Shen and C. H. Yan, *Chem. Eur. J.*, 2012, **18**, 5558.

S3. L. P. Liu, Z. B. Zhuang, T. Xie, Y. G. Wang, J. Li, Q. Peng and Y. D. Li, *J. Am. Chem. Soc.*, 2009, **131**, 16423.

S4. E. V. Shevchenko, D. V. Talapin, N. A. Kotov, S. O'Brien and C. B. Murray, *Nature*, 2006, **439**, 55.

S5. H. P. Zhou, C. H. Xu, W. Sun and C. H. Yan, *Adv. Funct. Mater.*, 2009, **19**, 3892.

S6. E. V. Shevchenko, D. V. Talapin, C. B. Murray and S. O'Brien, *J. Am. Chem. Soc.*, 2006, **128**, 3620.

S7. A. G. Dong, J. Chen, P. M. Vora, J. M. Kikkawa and C. B. Murray, *Nature*, 2010, **466**, 474.

S8. T. L. Wen and S. A. Majetich, *ACS Nano*, 2011, **5**, 8868.